Biochimica et Biophysica Acta 1828 (2013) 1441–1448

Contents lists available at SciVerse ScienceDirect

Biochimica et Biophysica Acta

journal homepage: www.elsevier.com/locate/bbamem

Lipid interaction triggering Septin2 to assembly into β-sheet structures investigated by Langmuir monolayers and PM-IRRAS

Julio C.P. Damalio [1], Thatyane M. Nobre [1], Jose Luiz Lopes, Osvaldo N. Oliveira Jr., Ana Paula U. Araújo *

Instituto de Física de São Carlos, Universidade de São Paulo (USP), Av. Trabalhador São-carlense, 400 São Carlos, SP, Brazil

ARTICLE INFO

Article history:
Received 5 December 2012
Received in revised form 17 January 2013
Accepted 6 February 2013
Available online 13 February 2013

Keywords:
Human septin 2
Langmuir monolayer
PM-IRRAS
Phospholipid
Amyloid

ABSTRACT

The molecular mechanisms responsible for protein structural changes in the central nervous system leading to Alzheimer's disease are unknown, but there is evidence that a family of proteins known as septins may be involved. Septins are a conserved group of GTP-binding proteins which participate in various cellular processes, including polarity determination and membrane dynamics. SEPT1, SEPT4, and SEPT2 have been found in deposits known as neurofibrillary tangles and glial fibrils in Alzheimer's disease. In this study, we provide molecular-level information for the interaction of SEPT2 with Langmuir monolayers at the air/water interface, which are used as simplified membrane models. The high surface activity of SEPT2 causes it to adsorb onto distinct types of lipid Langmuir monolayers, namely dipalmitoylphosphatidylcholine and PtdIns(4,5)P_2. However, the interaction with PtdIns(4,5)P_2 is much stronger, not only leading to a higher adsorption, but also to SEPT2 remaining inserted within the membrane at high surface pressures. Most importantly, in situ polarization-modulated infrared reflection absorption spectroscopy results indicated that the native secondary structure of SEPT2 is preserved upon interacting with PtdIns(4,5)P_2, but not when dipalmitoylphosphatidylcholine is at the air/water interface. Taken together, the results presented here suggest that the interaction between SEPT2 and the cell membrane may play an important role in the assembly of SEPT2 into amyloid-like fibers.

1. Introduction

Septins are members of a conserved group of GTP-binding proteins encountered in diverse eukaryotes [1], but originally discovered in yeast as being required for completion of the cell cycle [2]. They have been recognized as the fourth component of the cytoskeleton [3], playing important roles in multiple cellular processes in higher eukaryotes, most of which involve membrane association [4]. Their importance may be highlighted by several findings, as follows: SEPT4 and SEPT12 are present in the annulus, being essential for the integrity of mammalian spermatozoa [5,6]; SEPT7 is relevant for spine morphogenesis and dendrite development [7,8]; SEPT3 and SEPT5 play a role in synaptic vesicle traffic [9]; and SEPT2 and SEPT11 are required for phagosome formation [10]. Septins are known to assemble into high-order hetero-filaments and the following complexes were identified: SEPT2–SEPT6–SEPT7 [11], SEPT4–SEPT5–SEPT8 [12], SEPT7–SEPT11–SEPT9b [13], SEPT5–SEPT7–SEPT11 [14] and SEPT3–SEPT5–SEPT7 [15,16]. Recent reports mentioned the presence of SEPT9 associated to SEPT7 in the SEPT2–SEPT6–SEPT7 hetero-filament [17–19]. Contrasting to well-established septin hetero-filaments, some homo-filaments were observed, in vitro, in the case of SEPT2 [20] and SEPT4 [21], and these structures are believed to be amyloid-like [20,21].

Septins typically contain a variable N-terminal domain, a central GTP-binding domain and a C-terminal region [22], as illustrated in Fig. 1A. Towards the end of the N-terminal domain, most septins have a conserved polybasic region, responsible for lipid binding whose details remain unclear [23]. SEPT4 has been shown to bind directly to phosphatidylinositol (4,5)bisphosphate (PtdIns(4,5)P_2) and phosphatidylinositol (3,4,5)triphosphate (PtdIns(3,4,5)P_3), with a similar behavior being predicted for SEPT2 [23] because of its predominant isolation within the membrane fraction of fibroblasts [24]. In addition, the recombinant SEPT2–6–7 complex is able to modify the morphology of PC–PI giant liposome suspensions, inducing a tubulation process [25]. It has also been demonstrated that yeast septins not only bind phosphatidylinositol 4-phosphate and phosphatidylinositol 5-phosphate [26] but their association with PtdIns(4,5)P_2 promotes filament assembly [4,27].

SEPT2 was the first septin to have its structure solved [11], being essential for cytokinesis and found near the contractile ring. The microinjection of anti-SEPT2 results in binucleated cells [28]. It is also involved in pathologies such as brain tumors [29,30] and Alzheimer's disease [31]. Recently, we proposed that SEPT2 can assemble into amyloid filaments under specific in vitro conditions, though the precise mechanism has not been determined in detail [20]. A possible route to understanding amyloid assembly is to investigate the interaction

* Corresponding author. Tel.: +55 16 33739875; fax: +55 1633715381.
E-mail address: anapaula@ifsc.usp.br (A.P.U. Araújo).
[1] These authors contributed equally to this work.

0005-2736/$ – see front matter © 2013 Elsevier B.V. All rights reserved.
http://dx.doi.org/10.1016/j.bbamem.2013.02.003

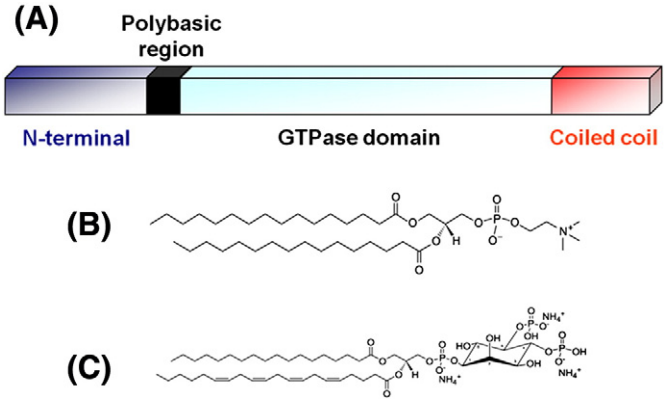

Fig. 1. Molecular structures. (A) The domain structure for SEPT2. SEPT2 has an N-terminal (blue) region comprising a polybasic region responsible for lipid binding (black), a GTPase domain (cyan), and a C-terminal domain (red). SEPT2 here refers to the whole protein, comprising all the structural domains. SEPT2NG and SEPT2G refer, respectively, to the GTPase domain plus the N-terminal domain (including the polybasic region) and GTPase domain alone [22]; (B) molecular structure of DPPC; (C) molecular structure of PtdIns(4,5)P_2. Lipid structures were modified from Avanti® Polar Lipids Inc. website.

between proteins and lipids in model membranes, for the lipid bilayer is believed to activate changes in the fibril kinetics [32–35]. For example, it is able to facilitate nucleation of Aβ fibrils, depending on the lipid composition [36]. Furthermore, liposomes have been shown to accelerate fibrillogenesis of the mutant N-terminal huntingtin fragment [37] and membrane binding is necessary for the exponential growth of prion protein aggregates [38]. Interestingly, under normal conditions, α-synuclein is predominantly bound to membranes in dopaminergic neurons, which minimizes aggregation. Indeed, significant reduction in the membrane-bound form of α-synuclein could result in pathological effects owing to α-synuclein aggregation [39]. Finally, β-amyloid proteins formed diffuse plaques that gradually developed into fibrillar amyloids upon interacting with membranes [40].

In spite of the considerable body of knowledge about SEPT2 and other septins, causal roles for amyloid formation have yet to be established. In this paper we investigate the binding of SEPT2 to PtdIns(4,5)P_2, compared with the phospholipid dipalmitoylphosphatidylcholine (DPPC), using the Langmuir monolayer technique. We also performed PM-IRRAS measurements to provide data on the secondary structure of SEPT2 during interaction with the Langmuir monolayer. Based on the results we propose a model through which binding to DPPC could trigger SEPT2 assembly into amyloid fibrils.

2. Materials and methods

2.1. Material and reagents

The lipids DPPC and PtdIns(4,5)P_2 shown in Fig. 1B and C were purchased from Avanti Polar Lipids and used without further purification. All other chemicals were obtained from Sigma and/or GE-Healthcare. Adsorption kinetics and surface pressure isotherms were obtained with a buffer solution of 25 mM Tris–HCl pH 7.8, containing 10% glycerol.

2.2. Protein expression and purification

The protein was obtained as described in [20], using a procedure briefly summarized as follows. *Escherichia coli* host strain BL21(DE3) containing the relevant *SEPT2* construct was grown at 37 °C and induced to produce the recombinant proteins at 18 °C. After centrifugation, the pelleted cells were re-suspended in the above-mentioned buffer, followed by sonication. The supernatant containing recombinant SEPT2 (whole protein, 1–361) was purified on nickel-affinity (QIAGEN) and Superdex-200 10/300 GL (GE-Healthcare) chromatography columns. The protein concentration was determined from its absorbance at 280 nm measured with a U-2001 Hitachi UV–visible spectrophotometer employing a theoretically determined extinction coefficient. The same procedure was adopted for SEPT2NG (1–308) and SEPT2G (35–308), referring respectively to the GTPase domain plus the N-terminal domain (including the polybasic region) and the GTPase domain alone.

2.3. Langmuir monolayers

Langmuir monolayers were prepared on a KSV (Minitrough model) Langmuir trough, housed in a class 10,000 clean room, equipped with a Wilhelmy plate made of filter paper. Chloroform solutions of DPPC and PtdIns(4,5)P_2 were spread on the buffer solution as aqueous subphase. Mixed monolayers containing SEPT2 were obtained by injecting a SEPT2 aqueous solution in the subphase, just below the interface, after lipid spreading. The SEPT2, SEPT2NG and SEPT2G final concentrations were 2 μM. Surface pressure–area (π–*A*) isotherms were obtained with a monolayer compression rate of 10 mm min^{-1}, including for pure proteins (absence of lipid). The adsorption kinetics of the proteins at a high lipid pressure (30 mN/m), corresponding to physiological biomembrane packing [41], was measured by injecting the protein solution under the interface and then monitoring the increase in surface pressure with time.

2.4. PM-IRRAS

Polarization-modulated infrared reflection absorption spectroscopy (PM-IRRAS) was performed using a KSV PMI 550 instrument (KSV instrument Ltd., Helsinki, Finland). The Langmuir trough is positioned with the light beam reaching the monolayer at a fixed incidence angle of ~80°, at which the intensity is maximum with a reduced noise level. Downward bands in the spectrum indicate transition moments oriented preferentially perpendicular to the surface, whereas upward absorption bands are assigned to transition moments oriented preferentially parallel to the surface plane. The incoming light is continuously modulated between s-polarization and p-polarization at a high frequency (50 kHz), which allows simultaneous measurement of the spectra for the two polarizations. The difference thus provides surface specific information, and the sum represents the reference spectrum. Since the spectra are measured simultaneously, the effect of water vapor is reduced. Measurements were performed at 20 °C and with SEPT2 (70 nM) heated at 37 °C for 30 min prior to the experiment. Lipids were spread at 5 mN/m and then SEPT2 was added to the subphase. The compression was performed every 5 mN/m up to a surface pressure of 40 mN/m.

2.5. Differential scanning calorimetry

Large unilamellar vesicles (LUVs) of pure DPPC and mixed DPPC/PtdIns(4,5)P_2 (95/5, mol/mol) were prepared by dissolving the dried lipids in a mixture of chloroform/methanol (2:1), then slowly removing the solvents with a nitrogen stream followed by 2 h evaporation in a SpeedVac system to yield a lipid film. The film was hydrated with Tris 25 mM (pH 7.8), 10% glycerol at 50 °C for 1 h and stirred in a vortex to produce the multilamellar vesicles that were further extruded with a 100 nm pore polycarbonate filter to yield the LUVs.

The thermotropic behavior of the LUVs of DPPC and DPPC/PtdIns(4,5)P_2 was investigated in a high-sensitivity VP-DSC microcalorimeter (MicroCal, Northampton, MA). DSC analyses were also recorded with the LUVs incubated with SEPT2 at a 500:1 and 1000:1 lipid/protein ratio. Samples were degassed and equilibrated for 15 min at 10 °C before each measurement, and scanned from 20 to 65 °C, with a 90 °C/hscan rate. Data acquisition, buffer subtraction and baseline

correction were performed with MicroCal Origin Software (version 7.0).

3. Results and discussion

3.1. Adsorption kinetics onto lipid monolayer

In this paper we investigated the adsorption of these three molecules, SEPT2, SEPT2NG and SEPT2G, onto a bare air/water interface and onto three types of lipid monolayer: DPPC, representing the phosphatidylcholine lipids, abundant in mammalian cell membranes, PtdIns(4,5)P_2, the phospholipid achieved to interact with some septins, and a mixture of PtdIns(4,5)P_2 (5%) and DPPC. The purpose was to determine which groups of SEPT2 are responsible for adsorption and interaction with membrane models. We stress that SEPT2, SEPT2NG and SEPT2G are always bound to GDP under the conditions adopted here, as confirmed in subsidiary experiments.

SEPT2, SEPT2NG and SEPT2G exhibited high surface activity, as shown in the insets in Fig. 2, indicating exposure of hydrophobic regions. This adsorption generated Gibbs monolayers for all molecules, which could be compressed up to ca. 50 mN/m. Furthermore, SEPT2, SEPT2NG and SEPT2G could also be incorporated into all the monolayers at low surface pressures (results not shown). Because our main interest is to study interaction at surface pressures corresponding to that prevailing in a cell membrane (i.e. 30–35 mN/m [41]), we concentrate on the results for a closely packed monolayer at 30 mN/m. We shall return to less packed monolayers while probing molecular structuring at the interface with PM-IRRAS. The adsorption of the proteins onto monolayers at 30 mN/m depended on the lipid at the air–water interface. Fig. 2 shows the changes in surface pressure, which represent the protein ability of altering lipid packing to allow for incorporation. Practically no incorporation was observed for DPPC for any of the molecules, with the pressure varying by only a few mN/m during the experiment. These small changes, including the apparently consistent decrease in pressure in Fig. 2A, could be related to the metastability of the monolayer, in addition to a slight instability caused by the guest molecules at such high surface pressures. In contrast, an efficient adsorption occurred for SEPT2 (Fig. 2A) and SEPT2NG (Fig. 2B) on PtdIns(4,5)P_2 and on a mixed monolayer of DPPC and PtdIns(4,5)P_2 (5%). For SEPT2NG, in particular, adsorption onto the PtdIns(4,5)P_2 monolayer was relatively slow in the beginning, for reason that it is not possible to determine, but then it was considerable after reaching equilibrium, which is most important for our discussion.

Fig. 2C indicates a minor incorporation of SEPT2G into PtdIns(4,5)P_2 and in the mixed DPPC + PtdIns(4,5)P_2 monolayers, but to a much smaller extent than for SEPT2 and SEPT2NG. These results represent the first experimental evidence of strong binding of human SEPT2 towards the PtdIns(4,5)P_2 lipid, especially because incorporation occurred even with only 5% of this lipid in the mixed monolayer. This could be expected from previous reports on the specificity towards PtdIns(4,5)P_2 in the case of human SEPT4 and the SEPT7–SEPT6–SEPT2 heterofilaments [23,25]. The strong interaction of SEPT2 and SEPT2NG for PtdIns(4,5)P_2 is attributed to the presence of a polybasic region towards the end of the N-terminal domain, which is also present in other human septins [23]. Indeed, for SEPT2G, which is the truncated form of SEPT2 lacking the N- and C-terminal domains, incorporation into the monolayers was much reduced, even though SEPT2G was surface active. This latter finding, inferred from the inset in Fig. 3, implies that the GTPase domain is the main region responsible for adsorption onto the air–water interface, which is consistent with the in vitro self-assembly of the SEPT2 GTPase domain into amyloid filaments [20].

The results with SEPT2 can be compared with those for the β-amyloid (Aβ) peptide, which also forms amyloid-like fibrils. The Aβ peptide adsorbed on the air–water interface, even for submicromolar concentrations, induced large changes in surface pressure, e.g. with 0.25 μM Aβ π was increased by ~13 mN/m [42].

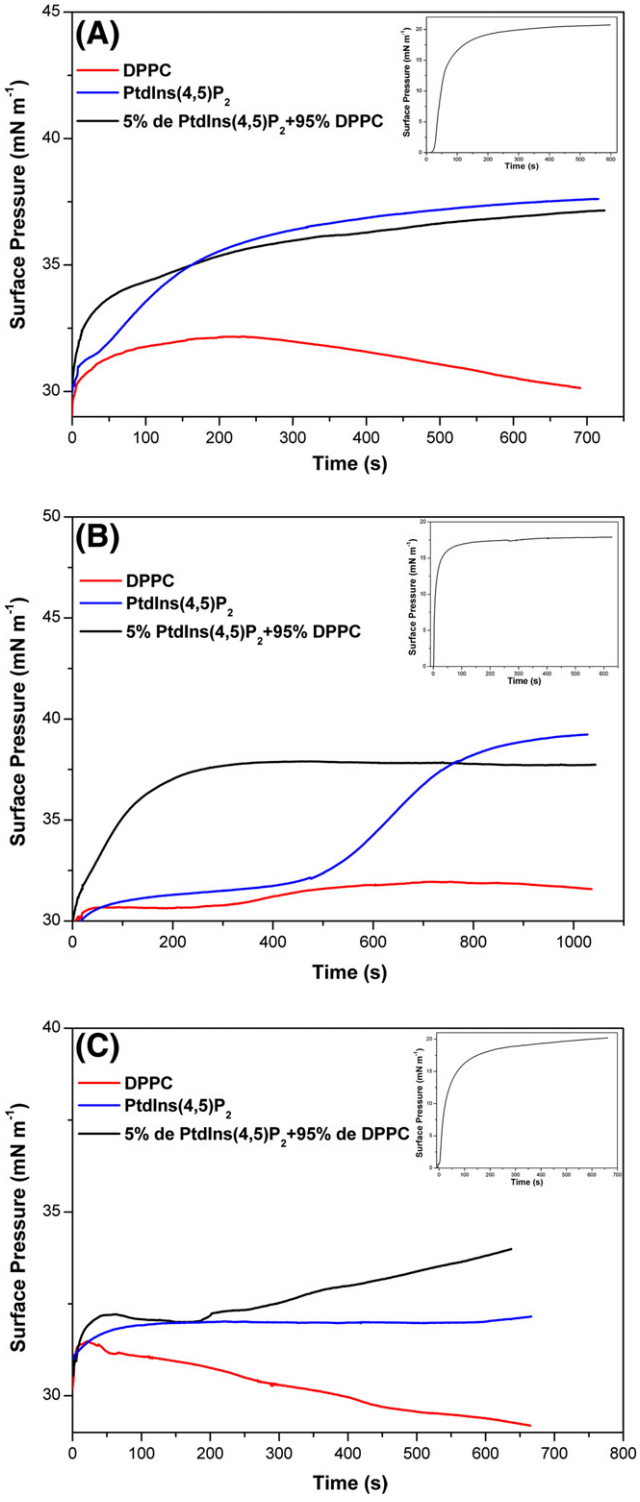

Fig. 2. Adsorption kinetics for SEPT2 (A), SEPT2NG (B) and SEPT2G (C) onto three monolayers (DPPC, PtdIns(4,5)P_2 and DPPC + PtdIns(4,5)P_2). The insets show the adsorption kinetics for a bare air/buffer interface. The DPPC curve in B shows a decreasing trend related to instability of the monolayer.

3.2. Secondary structure analysis by PM-IRRAS

While the surface pressure measurements could show unequivocally the adsorption properties of SEPT2, no information was obtained on its secondary structure at the interface. This could be performed with PM-IRRAS, which provides insights into the conformation of SEPT2 at the interface. We were particularly interested in determining whether

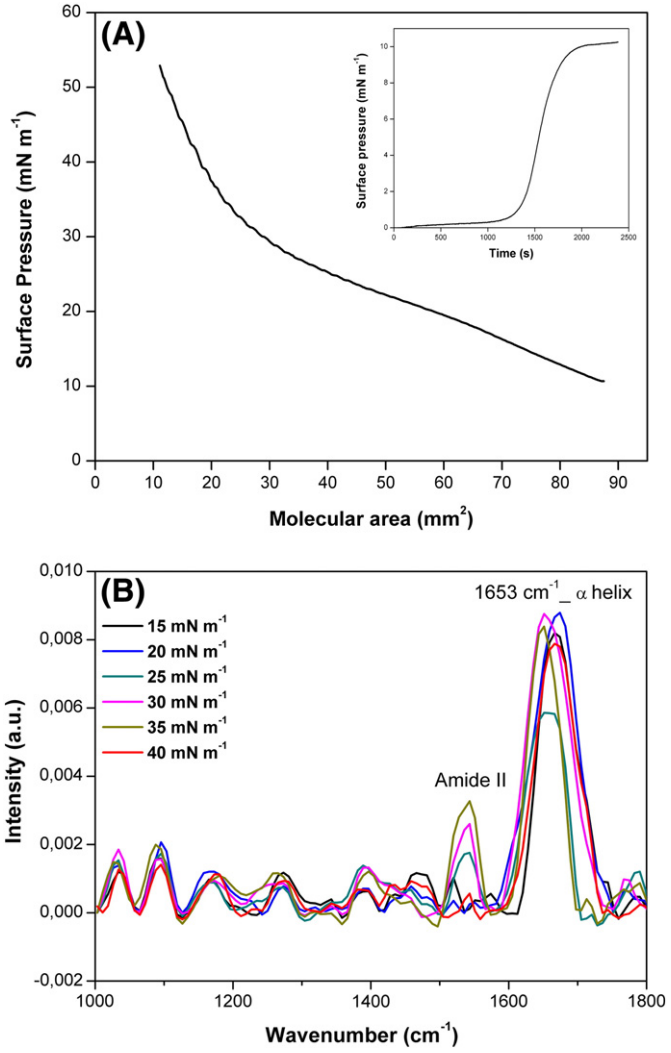

Fig. 3. SEPT2 adsorption at air/water interface and secondary structure analysis. (A) Surface pressure versus trough area isotherms. The inset represents the adsorption kinetics; (B) PM-IRRAS spectra for SEPT2 Gibbs monolayers. In (A) the trough area was used, instead of area per molecule because one does not know precisely the number of molecules at the interface in a Gibbs monolayer.

typical membrane lipids (represented by DPPC) and PtdIns(4,5)P_2, which were already shown to bind to SEPT2, play a significant role in the structuring of septins. SEPT2 presents the classic αβα sandwich architecture, where the α-helices are exposed at the surface while the β-sheets are buried in the protein structure (2QA5 PDB code) [11].

The PM-IRRAS spectra for a Gibbs monolayer of SEPT2 at the air/water interface, as shown in Fig. 3, feature two main bands, assigned to the amide I and amide II vibrations, centered at 1653 cm^{-1} and 1550 cm^{-1}, respectively. Since the position of the amide I band is sensitive to the polypeptide conformation, we infer that SEPT2 adopts predominantly an α-helical structure, consistent with circular dichroism data [20]. There are of course other components of secondary structures, but the protein region at the interface is primarily made of α-helices (one recalls that the PM-IRRAS technique is surface specific, and therefore only the adsorbed groups at the interface are detected). Interestingly, the intensity of the amide I band appears not to depend on the surface pressure, suggesting that the protein surface density was poorly altered with compression.

The incorporation of SEPT2 causes expansion on the surface pressure isotherm for a DPPC monolayer in Fig. 4A, as expected. Furthermore, the largest effects from SEPT2 occurred at low lipid packing, with the LE–LC phase transition being also affected. SEPT2 molecules incorporated onto the DPPC monolayer adopt a β-sheet structure predominantly, as indicated in the PM-IRRAS spectra in Fig. 4B. The intense band at 1624 cm^{-1} due to amide I (C═O) stretching is typical of β-sheets, which is also the case of the small band at 1698 cm^{-1} [43]. At high surface pressures, this band seems to merge into a broader band, at 1730 cm^{-1}. The band at 1550 cm^{-1} is assigned to the NH and CN bending (amide II) of the protein [43]. The conformational change from predominantly α-helices for SEPT2 adsorbed on a bare interface to β-sheets when adsorbed onto a DPPC monolayer is probably induced by exposure of a hydrophobic region with non-specific interaction with DPPC, and may be related to the assembling of amyloid structures. The band intensity increased with compression, indicating that the content of β-sheets is also increased. This is consistent with the amyloid proteins, which are rich in β-sheet content, parallel to the fiber axis [44].

These results are similar to those of the Aβ 1–40 peptide, which undergoes a conformational change while binding to brain lipid vesicles [36]. In addition, upon binding to cholesterol-dependent ganglioside clusters, the Aβ 1–42 protein changed from an α-helix-rich to a β-sheet-rich structure [45]. Another example of the influence of membrane composition in amyloid assembly is the conformational change from globular soluble to β-sheet enriched amyloid-like structure for the protein Glyceraldehyde-3-phosphate dehydrogenase, when it interacted with membranes containing anionic phospholipids [46].

The strong adsorption of SEPT2 onto pure PtdIns(4,5)P_2 monolayers, inferred from Fig. 2A, was confirmed in further experiments of adsorption kinetics and π–*A* isotherms in Fig. 4C. Most importantly, in contrast to the β-sheets observed when adsorbed onto a DPPC monolayer, SEPT2 adopts a predominant α-helical structure when incorporated onto the PtdIns(4,5)P_2 monolayer. This is illustrated in the PM-IRRAS spectra in Fig. 4D, with amide I and amide II bands at 1660 cm^{-1} and 1550 cm^{-1}, respectively. The native structure of SEPT2 was preserved upon monolayer compression, and therefore condensation of the film is not responsible for changes in the secondary structure.

Hence, the structural change to β-sheets must be attributed to the interaction with DPPC. It is possible that the protein region involved in the interaction depends on the lipid. The larger volume of the PtdIns(4,5)P_2 polar headgroup, compared with DPPC, maintains the protein hydrated at the water interface, rather than inserted amongst the hydrophobic tails. For PtdIns(4,5)P_2, the interaction is expected to occur via the polybasic region, exposed from the protein structure (2QA5 PDB code) while for DPPC insertion into the hydrophobic part of the membrane requires more significant rearrangement of the native structure. For the DPPC monolayer, we speculate that the interaction occurs via the exposed hydrophobic regions on the protein, which leads to filament formation. Since the interaction between SEPT2 and DPPC seems not to occur via polybasic region, the protein is forced to expose its hydrophobic portion, which might trigger the amyloidogenic process. In summary, the differences in SEPT2 binding to DPPC and PtdIns(4,5)P2 should be ascribed to the different regions of the protein interacting with the lipids.

In order to identify adsorption conditions of the amyloid filament, we performed PM-IRRAS experiments, depicted in Fig. 5, with SEPT2 pre-induced in the amyloid form. This was carried out by first inducing the homofilaments upon heating SEPT2 at 37 °C for 30 min [20]. These SEPT2 amyloid filaments adsorbed to a much lesser extent onto either a bare air/water interface or any of the monolayers studied (results not shown). The reduced incorporation onto a DPPC monolayer at 37 °C could be ascribed to: i) difficulty in penetrating the monolayer owing to the size of the homofilaments since the interactions are non-specific; or ii) the protein hydrophobic regions responsible for interaction at the interface which are now involved in the filament formation.

The injection of SEPT2 in the form of fibers into the subphase of a closely-packed PtdIns(4,5)P_2 monolayer (at 30 mN/m) led to no

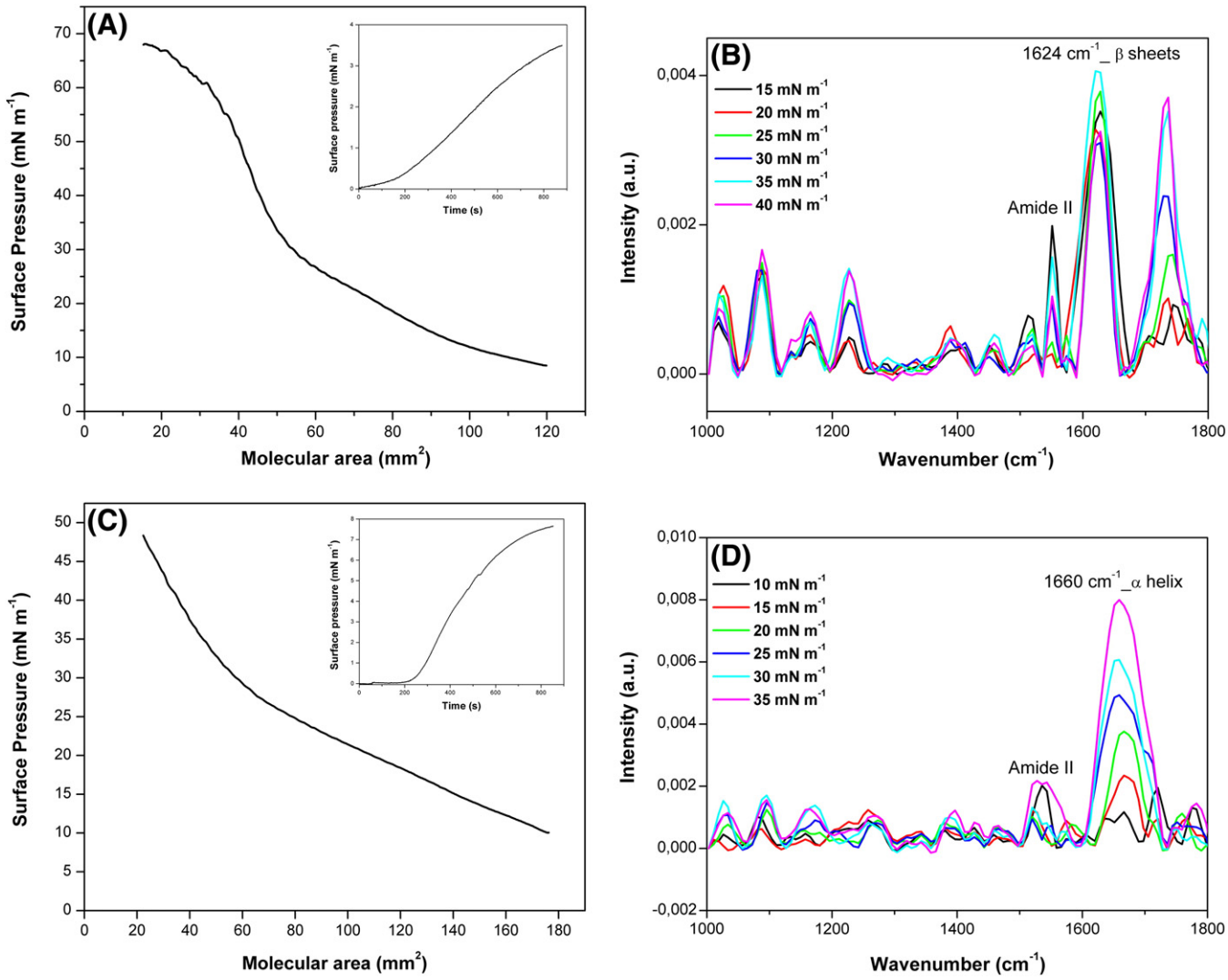

Fig. 4. Protein adsorption at monolayer and secondary structure analysis. (A) Surface pressure versus trough area isotherm in a DPPC monolayer. The inset represents the adsorption kinetics; (B) PM-IRRAS spectra for SEPT2 adsorbed on DPPC monolayers at various surface pressures; (C) surface pressure versus trough area isotherm in a PtdIns(4,5)P_2 monolayer. The inset represents the adsorption kinetics; (D) PM-IRRAS spectra for SEPT2 adsorbed on a PtdIns(4,5)P_2 monolayer at various surface pressures.

increase in surface pressure. Therefore, the specificity of SEPT2 in the amyloid form was not relevant for this lipid. This is additional evidence of the interplay between these two processes: interaction with the membrane and formation of fibrils.

3.3. Differential scanning calorimetry analyses

In order to verify the adsorption of SEPT2 in large unilamellar vesicles containing the PtdIns(4,5)P_2, DSC analyses were employed. Firstly, the incorporation of 5% PtdIns(4,5)P_2 into the DPPC vesicles was probed. Fig. 6 shows the thermotropic behavior of the LUVs of DPPC and DPPC/PtdIns(4,5)P_2. Consistent with the literature [47,48], the temperature for the gel to liquid-crystalline phase transition in DPPC vesicles was centered at 41.7 °C, with a single sharp endothermic peak. Similarly, the DSC thermogram for the mixed vesicles also presented a single but broader peak, with the main phase transition centered at 41.3 °C, indicating that incorporation of PtdIns(4,5)P_2 into the pure DPPC vesicles has slightly shifted the main transition. Therefore, since no additional peaks were observed in the thermograms for the vesicles with PtdIns(4,5)P_2, and the $\Delta T_{1/2}$ value for pure DPPC vesicles increased, both lipids must have been incorporated into the same bilayer. Otherwise, two transitions corresponding to DPPC and PtdIns(4,5)P_2 would be observed [49].

Secondly, to evaluate whether the incorporation of SEPT2 into the LUVs was affected by the presence of the PtdIns(4,5)P_2, DSC analyses in vesicles with and without the PtdIns(4,5)P_2 were performed, using two different lipid/protein molar ratios. When SEPT2 was incubated with the LUVs of pure DPPC (Figure 6A), no significant changes in the thermodynamic parameters were observed. There was only a slight increase in the ΔH and a broadening of the transition peak was observed when the protein/lipid ratio increased, indicating that the protein interacts weakly with the zwitterionic phospholipid, in agreement with the low adsorption of SEPT2 in the DPPC monolayers observed in this paper.

In contrast, in the presence of 5% PtdIns(4,5)P_2 in the LUVs, the effects promoted by SEPT2 were an increase in enthalpy of 44% and a broadening of the main transition peak to 1.33 °C (Fig. 6B). These effects were shown to depend on the amount of SEPT2 added to the vesicles, since both were proportional to the increase in the protein/lipid ratio. These effects are characteristic of hydrophilic molecules whose interaction with phospholipid vesicles depends strongly on electrostatic binding, in which minimal and superficial effects are produced on the vesicles. The final result is an increase in the transition enthalpy while the Tm can either be unaltered or increased slightly, especially due to a lack of liposome penetration [50]. The interaction of ribonuclease and polylysine with DPPC or DPPG vesicles

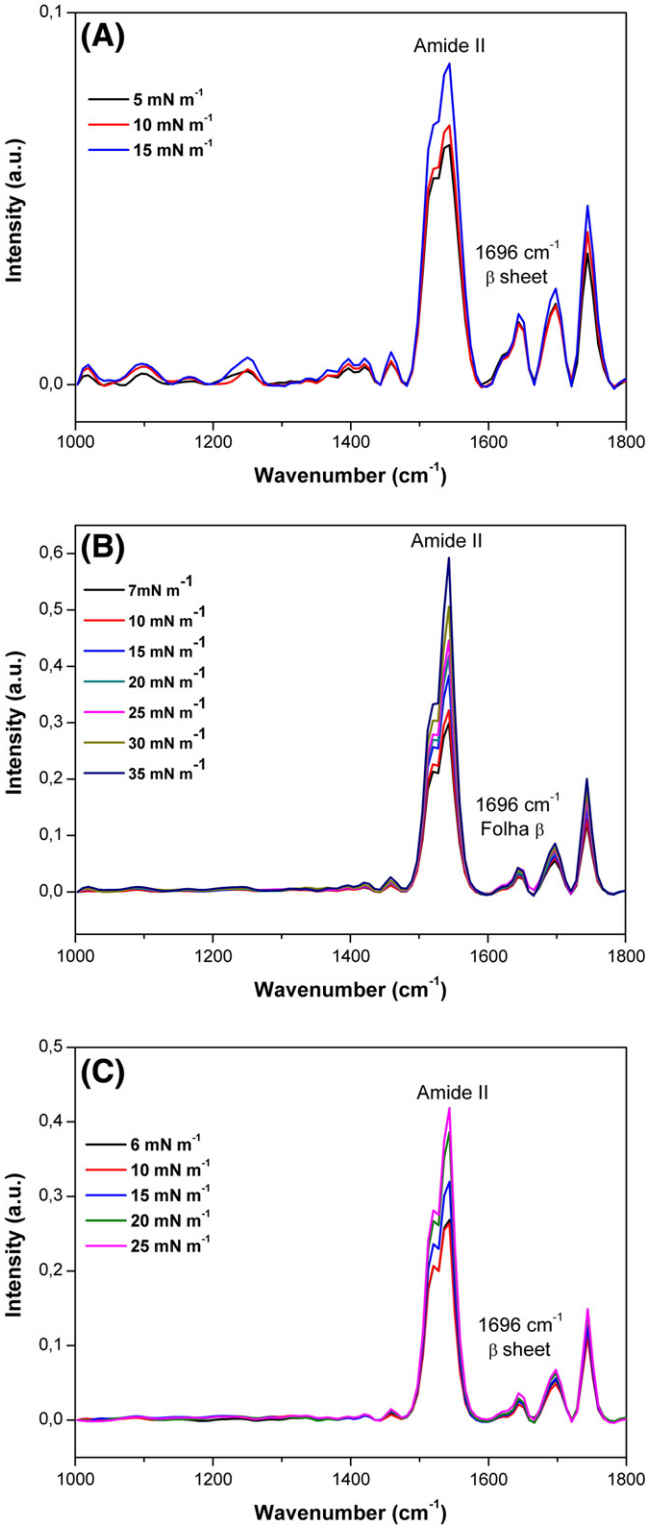

Fig. 5. PM-IRRAS spectra of SEPT2 in fibril form at 37 °C. (A) SEPT2 at air/water interface; (B) SEPT2 at DPPC monolayer; (C) SEPT2 at PtdIns(4,5)P_2 monolayer.

exemplifies this type of interaction [50,51]. It was demonstrated that these interactions are indicative of simple surface binding of the protein on the lipid bilayer without penetration into the hydrocarbon region.

As discussed previously, the surface interaction between SEPT2 and DPPC/PtdIns(4,5)P_2 vesicles could be electrostatic, involving the polybasic region of the protein and the negatively charged head of

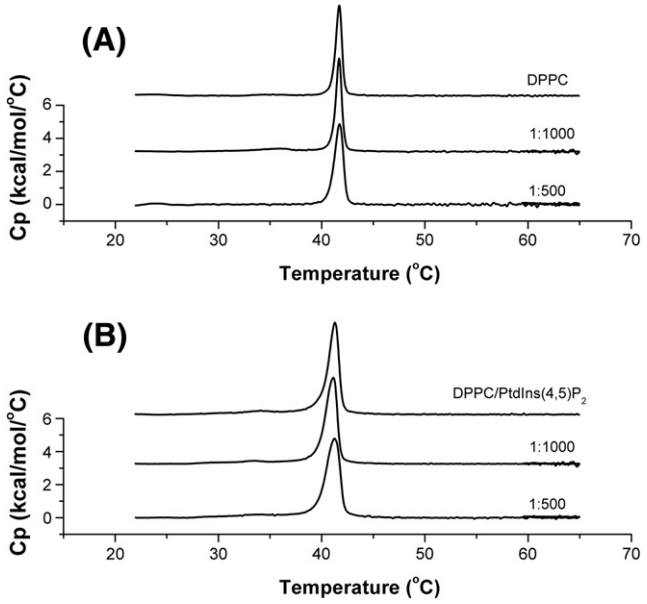

Fig. 6. DSC heating scans of the effect of SEPT2 on the thermotropic phase behavior. (A) Pure DPPC vesicles; (B) mixed DPPC/PtdIns(4,5)P_2 (95:5, mol/mol) vesicles. The values on each curve refer to the SEPT2 to lipid molar ratio.

the PtdIns(4,5)P_2. The thermodynamic parameters, such as the values for the main phase transition temperatures (Tm) and enthalpies (ΔH), are summarized in Table 1.

3.4. Possible model for SEPT2 interaction with membrane models

In order to conceive a model which incorporated aspects of both membrane–protein interaction and the formation of amyloid filaments, we summarize the main findings from the results above, as follows.

SEPT2 interacts specifically with PtdIns(4,5)P_2, remaining incorporated in the monolayer even at high surface pressures (corresponding to a real membrane), and with its secondary structure preserved. The anchoring is probably via the polybasic region in the N-terminal domain, since similar results were obtained for the whole protein SEPT2 and its truncated form SEPT2NG (which preserves the N-terminal domain), but little incorporation was observed for SEPT2G (which lacks it).

The proteins (SEPT2, SEPT2NG and SEPT2G) cannot be incorporated into closely packed DPPC monolayers. When SEPT2 is adsorbed onto a DPPC monolayer at a low surface pressure, the protein loses its native conformation (going from a predominantly α-helical structure to one dominated by β-sheets) during monolayer compression. The difference in behavior may be attributed to presence of the polybasic helix, which maintains the protein interacting at the surface of lipid monolayer. Additionaly, if SEPT2 is pre-induced to form amyloid filaments before being injected in the subphase, it can no longer interact with PtdIns(4,5)P_2 in the Langmuir monolayer.

From these findings, one may infer that SEPT2 molecules will form amyloid filaments if they have no access to PtdIns(4,5)P_2 for anchoring

Table 1
Thermodynamic parameters for interaction of SEPT2 with pure DPPC and mixed DPPC/PtdIns(4,5)P2 (95/5, mol/mol) vesicles.

	Protein/lipid ratio	T_m (°C)	$\Delta T_{1/2}$ (°C)	ΔH (kcal/mol)
DPPC	–	41.7	0.71	5.42
	1:1000	41.7	0.66	5.59
	1:500	41.7	1.02	5.62
DPPC/PtdIns(4,5)P_2	–	41.3	1.16	7.84
	1:1000	41.2	1.33	9.03
	1:500	41.3	1.57	9.15

to the membrane via the polybasic region. Furthermore, once filaments are formed no further incorporation into the membrane is possible.

4. Conclusions

A large number of biological processes occur in the membranes, involving mostly proteins and lipids [52]. For example, PtdIns(4,5)P_2 controls various aspects of the cell cytoskeleton, including actin dynamics at the cell membrane [53,54]. SEPT2 has a polybasic region, which is considered responsible for binding to PtdIns(4,5)P_2 [23]. Here we have demonstrated the particular interaction of SEPT2 (and SEPT2NG) with PtdIns(4,5)P_2, and the crucial role played by the polybasic region. Some septins are also related to neurodegenerative diseases, as is the case of SEPT2 in Alzheimer's disease [20,31]. Studies have revealed that the conformation and aggregation states of the amyloidogenic protein are influenced by the interaction with lipid membranes and that the lipid bilayer actively changes fibril kinetics [32–35]. This may also be the case for SEPT2 amyloid assembly, which is triggered by the interaction with DPPC.

The evidence shown in this study broadly supports the notion of physiological interactions between SEPT2 and PtdIns(4,5)P_2, which serve to maintain the native structure of the protein. These may well be relevant to the formation and stabilization of native septin filaments (be they hetero- or homo-filaments) essential for biological activity. Interaction with DPPC, on the other hand, may lead to structural perturbation of the protein with pathological consequences in the form of amyloid deposits.

Acknowledgements

The authors thank Professor Richard Charles Garratt for critical reading of the manuscript. This work was supported by the FAPESP, the CNPq and the CAPES (Brazil).

References

[1] E.T. Spiliotis, M. Kinoshita, W.J. Nelson, A mitotic septin scaffold required for mammalian chromosome congression and segregation, Science 307 (2005) 1781–1785.
[2] L.H. Hartwell, Genetic control of the cell division cycle in yeast. IV. Genes controlling bud emergence and cytokinesis, Exp. Cell Res. 69 (1971) 265–276.
[3] S. Mostowy, P. Cossart, Septins: the fourth component of the cytoskeleton, Nat. Rev. Mol. Cell Biol. 13 (2012) 183–194.
[4] A. Bertin, M.A. McMurray, L. Thai, G. Garcia, V. Votin, P. Grob, T. Allyn, J. Thorner, E. Nogales, Phosphatidylinositol-4,5-bisphosphate promotes budding yeast septin filament assembly and organization, J. Mol. Biol. 404 (2010) 711–731.
[5] M. Ihara, A. Kinoshita, S. Yamada, H. Tanaka, A. Tanigaki, A. Kitano, M. Goto, K. Okubo, H. Nishiyama, O. Ogawa, C. Takahashi, O. Ogawa, C. Takahashi, S. Itohara, Y. Nishimune, M. Noda, M. Kinoshita, Cortical organization by the septin cytoskeleton is essential for structural and mechanical integrity of mammalian spermatozoa, Dev. Cell 8 (2005) 343–352.
[6] J.D. Steels, M.R. Estey, C.D. Froese, D. Reynaud, C. Pace-Asciak, W.S. Trimble, Sept12 is a component of the mammalian sperm tail annulus, Cell Motil. Cytoskeleton 64 (2007) 794–807.
[7] T. Tada, A. Simonetta, M. Batterton, M. Kinoshita, D. Edbauer, M. Sheng, Role of septin cytoskeleton in spine morphogenesis and dendrite development in neurons, Curr. Biol. 17 (2007) 1752–1758.
[8] Y.L. Xie, J.P. Vessey, A. Konecna, R. Dahm, P. Macchi, M.A. Kiebler, The GTP-binding protein septin 7 is critical for dendrite branching and dendritic-spine morphology, Curr. Biol. 17 (2007) 1746–1751.
[9] C.W. Tsang, M. Fedchyshyn, J. Harrison, H. Xie, J. Xue, P.J. Robinson, L.Y. Wang, W.S. Trimble, Superfluous role of mammalian septins 3 and 5 in neuronal development and synaptic transmission, Mol. Cell. Biol. 28 (2008) 7012–7029.
[10] Y.W. Huang, M. Yan, R.F. Collins, J.E. Diciccio, S. Grinstein, W.S. Trimble, Mammalian septins are required for phagosome formation, Mol. Biol. Cell 19 (2008) 1717–1726.
[11] M. Sirajuddin, M. Farkasovsky, F. Hauer, D. Kuhlmann, I.G. Macara, M. Weyand, H. Stark, A. Wittinghofer, Structural insight into filament formation by mammalian septins, Nature 449 (2007) 311–315.
[12] C. Martinez, M.A. Sanjuan, J.A. Dent, L. Karlsson, J. Ware, Human septin–septin interactions as a prerequisite for targeting septin complexes in the cytosol, Biochem. J. 382 (2004) 783–791.
[13] K. Nagata, T. Asano, Y. Nozawa, M. Inagaki, Biochemical and cell biological analyses of a mammalian septin complex, Sept7/9b/11, J. Biol. Chem. 279 (2004) 55895–55904.
[14] P. Macchi, Y.L. Xie, J.P. Vessey, A. Konecna, R. Dahm, M.A. Kiebler, The GTP-binding protein septin 7 is critical for dendrite branching and dendritic-spine morphology, Curr. Biol. 17 (2007) 1746–1751.
[15] M. Kengaku, K. Fujishima, H. Kiyonari, J. Kurisu, T. Hirano, Targeted disruption of Sept3, a heteromeric assembly partner of Sept5 and Sept7 in axons, has no effect on developing CNS neurons, J. Neurochem. 102 (2007) 77–92.
[16] J. Trinick, N. Lukoyanova, S.A. Baldwin, 3D reconstruction of mammalian septin filaments, J. Mol. Biol. 376 (2008) 1–7.
[17] M. Nakahira, J.N.A. Macedo, T.V. Seraphim, N. Cavalcante, T.A.C.B. Souza, J.C.P. Damalio, L.F. Reyes, E.M. Assmann, M.R. Alborghetti, R.C. Garratt, A.P.U. Araujo, N.I.T. Zanchin, J.A.R.G. Barbosa, J. Kobarg, A draft of the human septin interactome, PLoS One 5 (2010) e0013799.
[18] K. Sandrock, I. Bartsch, S. Blaser, A. Busse, E. Busse, B. Zieger, Characterization of human septin interactions, Biol. Chem. 392 (2011) 751–761.
[19] M.E. Sellin, L. Sandblad, S. Stenmark, M. Gullberg, Deciphering the rules governing assembly order of mammalian septin complexes, Mol. Biol. Cell (2011) 3152–3164.
[20] J.C. PissutiDamalio, W. Garcia, J.N. Alves Macedo, I. de Almeida Marques, J.M. Andreu, R. Giraldo, R.C. Garratt, A.P. Ulian Araujo, Self assembly of human septin 2 into amyloid filaments, Biochimie (2011) 628–636.
[21] W. Garcia, A.P.U. de Araujo, F. Lara, D. Foguel, M. Tanaka, T. Tanaka, R.C. Garratt, An intermediate structure in the thermal unfolding of the GTPase domain of human septin 4 (SEPT4/Bradeion-beta) forms amyloid-like filaments in vitro, Biochemistry 46 (2007) 11101–11109.
[22] B. Kartmann, D. Roth, Novel roles for mammalian septins: from vesicle trafficking to oncogenesis, J. Cell Sci. 114 (2001) 839–844.
[23] J. Zhang, C. Kong, H. Xie, P.S. McPherson, S. Grinstein, W.S. Trimble, Phosphatidylinositol polyphosphate binding to the mammalian septin H5 is modulated by GTP, Curr. Biol. 9 (1999) 1458–1467.
[24] H. Xie, M. Surka, J. Howard, W.S. Trimble, Characterization of the mammalian septin H5: distinct patterns of cytoskeletal and membrane association from other septin proteins, Cell Motil. Cytoskeleton 43 (1999) 52–62.
[25] Y. Tanaka-Takiguchi, M. Kinoshita, K. Takiguchi, Septin-mediated uniform bracing of phospholipid membranes, Curr. Biol. 19 (2009) 140–145.
[26] A. Casamayor, M. Snyder, Molecular dissection of a yeast septin: distinct domains are required for septin interaction, localization, and function, Mol. Cell. Biol. 23 (2003) 2762–2777.
[27] A. Bertin, M.A. McMurray, J. Piersonb, L. Thai, K.L. McDonald, E.A. Zehr, G. Garcia, P. Peters, J. Thorner, E. Nogales, Three-dimensional ultrastructure of the septin filament network in *Saccharomyces cerevisiae*, Mol. Biol. Cell 23 (2012) 423–432.
[28] M. Kinoshita, S. Kumar, A. Mizoguchi, C. Ide, A. Kinoshita, T. Haraguchi, Y. Hiraoka, M. Noda, Nedd5, a mammalian septin, is a novel cytoskeletal component interacting with actin-based structures, Genes Dev. 11 (1997) 1535–1547.
[29] A.A. Khalil, P. James, Biomarker discovery: a proteomic approach for brain cancer profiling, Cancer Sci. 98 (2007) 201–213.
[30] K. Sakai, M. Kurimoto, A. Tsugu, S.L. Hubbard, W.S. Trimble, J.T. Rutka, Expression of Nedd5, a mammalian septin, in human brain tumors, J. Neurooncol 57 (2002) 169–177.
[31] A. Kinoshita, M. Kinoshita, H. Akiyama, H. Tomimoto, I. Akiguchi, S. Kumar, M. Noda, J. Kimura, Identification of septins in neurofibrillary tangles in Alzheimer's disease, Am. J. Pathol. 153 (1998) 1551–1560.
[32] R.M. Murphy, Kinetics of amyloid formation and membrane interaction with amyloidogenic proteins, Biochim. Biophys. Acta Biomembr. 1768 (2007) 1923–1934.
[33] D.J. Selkoe, Cell biology of protein misfolding: the examples of Alzheimer's and Parkinson's diseases, Nat. Cell Biol. 6 (2004) 1054–1061.
[34] C. Haass, D.J. Selkoe, Soluble protein oligomers in neurodegeneration: lessons from the Alzheimer's amyloid beta-peptide, Nat. Rev. Mol. Cell Biol. 8 (2007) 101–112.
[35] G.P. Gorbenko, P.K. Kinnunen, The role of lipid–protein interactions in amyloid-type protein fibril formation, Chem. Phys. Lipids 141 (2006) 72–82.
[36] C.M. Yip, J. McLaurin, Amyloid-beta peptide assembly: a critical step in fibrillogenesis and membrane disruption, Biophys. J. 80 (2001) 1359–1371.
[37] J. Suopanki, C. Gotz, G. Lutsch, J. Schiller, P. Harjes, A. Herrmann, E.E. Wanker, Interaction of huntingtin fragments with brain membranes — clues to early dysfunction in Huntington's disease, J. Neurochem. 96 (2006) 870–884.
[38] D.L. Cox, R.R.P. Sing, S.C. Yang, Prion disease: exponential growth requires membrane binding, Biophys. J. 90 (2006) L77–L79.
[39] M. Zhu, A.L. Fink, Lipid binding inhibits alpha-synuclein fibril formation, J. Biol. Chem. 278 (2003) 16873–16877.
[40] H. Yamaguchi, M.L.C. Maat-Schieman, S.G. van Duinen, F.A. Prins, P. Neeskens, R. Natte, R.A.C. Roos, Amyloid beta protein (A beta) starts to deposit as plasma membrane-bound form in diffuse plaques of brains from hereditary cerebral hemorrhage with amyloidosis-Dutch type, Alzheimer disease and nondemented aged subjects, J. Neuropathol. Exp. Neurol. 59 (2000) 723–732.
[41] W. Caetano, M. Ferreira, M. Tabak, M.I.M. Sanchez, O.N. Oliveira, P. Kruger, M. Schalke, M. Losche, Cooperativity of phospholipid reorganization upon interaction of dipyridamole with surface monolayers on water, Biophys. Chem. 91 (2001) 21–35.
[42] D.L. Jiang, K.L. Dinh, T.C. Ruthenburg, Y. Zhang, L. Su, D.P. Land, F.M. Zhou, A kinetic model for beta-amyloid adsorption at the air/solution interface and its implication to the beta-amyloid aggregation process, J. Phys. Chem. B 113 (2009) 3160–3168.
[43] C. Pasquini, Near infrared spectroscopy: fundamentals, practical aspects and analytical applications, J. Braz. Chem. Soc. 14 (2003) 198–219.
[44] R. Nelson, D. Eisenberg, Structural models of amyloid-like fibrils, Fibrous Proteins: Amyloids, Prions and Beta Proteins, 73, 2006, pp. 235–282.
[45] M. Wakabayashi, K. Matsuzaki, Formation of amyloids by Abeta-(1–42) on NGF-differentiated PC12 cells: roles of gangliosides and cholesterol, J. Mol. Biol. 371 (2007) 924–933.
[46] H.X. Zhao, E.K.J. Tuominen, P.K.J. Kinnunen, Formation of amyloid fibers triggered by phosphatidylserine-containing membranes, Biochemistry 43 (2004) 10302–10307.
[47] S. Tristram-Nagle, J.F. Nagle, Lipid bilayers: thermodynamics, structure, fluctuations, and interactions, Chem. Phys. Lipids 127 (2004) 3–14.

[48] C. Demetzos, Differential scanning calorimetry (DSC): a tool to study the thermal behavior of lipid bilayers and liposomal stability, J. Liposome Res. 18 (2008) 159–173.
[49] J.M. Boggs, D.D. Wood, M.A. Moscarello, D. Papahadjopoulos, Lipid phase separation induced by a hydrophobic protein in phosphatidylserine–phosphatidylcholine vesicles, Biochemistry 16 (1977) 2325–2329.
[50] D. Papahadjopoulos, M. Moscarello, E.H. Eylar, T. Isac, Effects of proteins on thermotropic phase-transitions of phospholipid membranes, Biochim. Biophys. Acta 401 (1975) 317–335.
[51] Y.L. Lo, Y.E. Rahman, Protein location in liposomes, a drug carrier — a prediction by differential scanning calorimetry, J. Pharm. Sci. 84 (1995) 805–814.
[52] W.R. Glomm, S. Volden, O. Halskau, M.H. Ese, Same system-different results: the importance of protein-introduction protocols in Langmuir-monolayer studies of lipid–protein interactions, Anal. Chem. 81 (2009) 3042–3050.
[53] D. Raucher, T. Stauffer, W. Chen, K. Shen, S.L. Guo, J.D. York, M.P. Sheetz, T. Meyer, Phosphatidylinositol 4,5-bisphosphate functions as a second messenger that regulates cytoskeleton–plasma membrane adhesion, Cell 100 (2000) 221–228.
[54] A.S. Sechi, J. Wehland, The actin cytoskeleton and plasma membrane connection: PtdIns(4,5)P-2 influences cytoskeletal protein activity at the plasma membrane, J. Cell Sci. 113 (2000) 3685–3695.